Lattice Plane Response during Tensile Loading of an Aluminum 2 Percent Magnesium Alloy

B. CLAUSEN and M.A.M. BOURKE

In-situ neutron diffraction measurements of plane specific elastic lattice strains were made during a tensile test of an aluminum 2 pct magnesium alloy. The macroscopic response exhibited a serrated flow curve, evidence of dynamic strain aging. The neutron results are compared to calculations using a self-consistent polycrystal deformation model. The relatively poor agreement with the measured data may suggest that the model has limitations with respect to face-centered cubic (fcc) alloys with low elastic anisotropy.

I. INTRODUCTION

THE residual strain state in aluminum and aluminum alloys has previously been studied using neutron diffraction measurements[1,2,3] and also during loading.[4,5,6] In the present work, the development of lattice strains for eight reflections, both parallel and perpendicular to the tensile axis, are reported for tensile testing of an aluminum 2 pct magnesium alloy. The chemical composition of the material is given in Table I.

The data were obtained using pulsed neutrons and the time-of-flight technique, thus lattice spacings for multiple reflections were readily available. Results are reported for the unique (i.e. excluding second order, unresolved and overlapping reflections) reflections up to the 531 reflection, which is the first reflection with lowest possible symmetry in the face-centered cubic (fcc) lattice. The procedure is described in more detail in Reference 7 for an investigation of lattice strain development in an austenitic stainless steel.

In contrast to stainless steel, aluminum is highly isotropic in its elastic response ($2C_{44}/(C_{11} - C_{12}) = 1.22$ for aluminum compared to 3.21 for stainless steel), thus the spread between reflections is expected to be much smaller than in stainless steel, at least in the elastic region. The accuracy of a neutron diffraction strain measurement is generally about $\pm$ 50 $\mu\varepsilon$ (microstrain or 10^{-6} strain) and the elastic strain at yield in our earlier work on commercially pure aluminum[4] was about 250 $\mu\varepsilon$ yielding an accuracy of about $\pm$ 20 pct of the elastic strain at yield. In an attempt to improve our strain resolution with regard to the yield strain, we opted to use an aluminum alloy (2 pct Mg) that exhibits an elastic strain before yield of about 500 $\mu\varepsilon$. However, as described in Section II, the introduction of magnesium in the aluminum lattice resulted in dynamic strain aging (DSA).

II. EXPERIMENTAL PROCEDURE

The neutron diffraction measurements were made at the Manuel Lujan Jr. Neutron Scattering Center, Los Alamos National Laboratory, using the neutron powder diffraction instrument. The procedure for *in-situ* loading experiments is outlined elsewhere.[8]

The material under study was a cast aluminum 2 pct magnesium alloy that was annealed at 400 °C for 15 minutes prior to the *in-situ* neutron diffraction measurements. The average grain size was 112 μm and the grains were fairly equiaxed, as seen in the optical micrograph in Figure 1. During the neutron diffraction measurements, lattice plane spacings were measured parallel and perpendicular to the tensile axis using detector banks at $\pm$ 90 deg to the incident beam. Each detector subtends 11 deg 2θ over which the diffracted data are integrated, corresponding to an "average" in the strain direction of $\pm$ 5.5 deg.

The sample, a threaded end ASTM standard specimen,[9] was held at constant stress for up to 3 hours at a series of static tensile loads, while neutron measurements were made. The macroscopic response is shown in Figure 2. The vertical steps in the measured stress-strain curve are elastic loading followed by increments of plastic deformation (horizontal steps). This behavior is indicative of DSA. During the elastic loading, dislocations are arrested by the magnesium atoms in the aluminum lattice. The plastic relaxation occurs when the driving force for the dislocations becomes larger than a given threshold and the dislocations can move past the magnesium atoms.[10] No DSA was observed during the holds while the diffraction data were collected. The measurements were performed under load control. Even at room temperature, some relaxation was observed during the neutron measurements, but by using a constant stress (load) on the sample, the lattice spacing should remain constant during the measurement.

Lattice strains as a function of applied load are reported for directions parallel and perpendicular to the tensile axis from the measurements (Figure 3) and from the self-consistent model calculations (Figure 4). The quoted stresses and strains are relative to a nominal load of 5 MPa (used to hold the sample in position). Starting from a nominal tensile stress is preferable since it precludes any small backlash on uptake of the stress that might result in small realignment of the sample. If the sample moves during a measurement, systematic effects associated with the change in scattering geometry can introduce significant apparent strains. The load levels for the neutron measurements are indicated by the symbols in Figure 1 and for the 420 reflection in Figure 3. Error bars

B. CLAUSEN, Postdoctoral Research Associate, and M.A.M. BOURKE, Technical Staff Member, are with the Los Alamos National Laboratory, Los Alamos, NM 87545.

Manuscript submitted May 2, 2000.

U.S. GOVERNMENT WORK
NOT PROTECTED BY U.S. COPYRIGHT

Table I. Chemical Composition (Weight Percent) of the Aluminum 2 Percent Magnesium Alloy

	Fe	Si	Cu	Mn	Cr	Ti	Mg
Aluminum 2 pct magnesium	<0.001	<0.005	<0.002	<0.001	<0.005	0.011	2.04

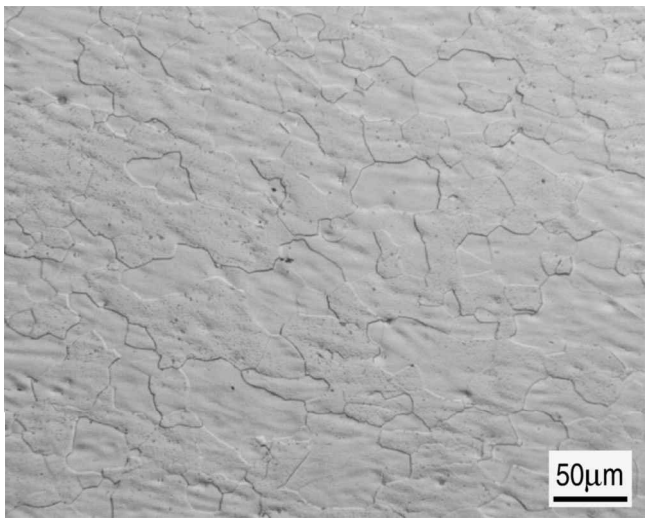

Fig. 1—Micrograph from a cross section of the aluminum alloy taken after the tensile test. The sample was prepared for optical microscopy by etching with Tuckers regent (15 mL HF, 45 mL HCl, 5 mL HNO_3, and 25 mL H_2O).

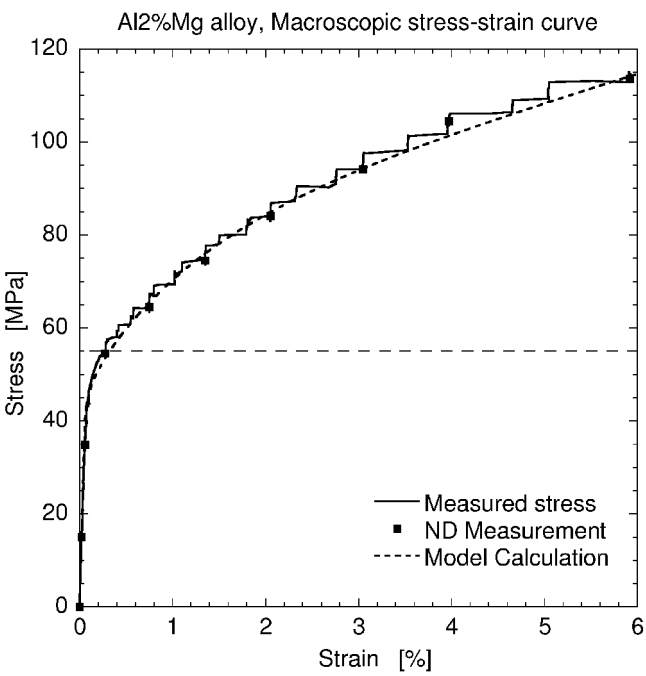

Fig. 2—Measured and calculated macroscopic stress-strain curves for the aluminum 2 pct magnesium alloy. The symbols indicate the load levels for the neutron diffraction measurements. The horizontal dotted line shows the $\sigma_{0.2\ pct}$ yield limit.

for the measurements are also indicated for the 420 reflection in Figure 3.

III. SELF-CONSISTENT POLYCRYSTAL DEFORMATION MODEL

The model used to calculate the elastic lattice strain response for grain subsets represented by the reflections in

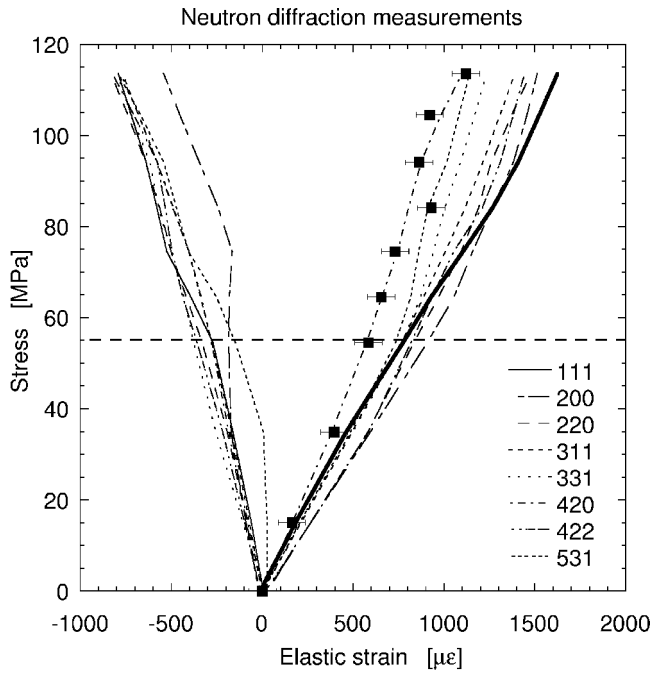

Fig. 3—Measured elastic lattice strains parallel and perpendicular to the tensile axis *vs* the applied stress. To illustrate the quality of the data, data points and error bars are shown for the 420 reflection parallel to the tensile axis. Smooth fits are shown for all other reflections. The horizontal dotted line shows the $\sigma_{0.2\ pct}$ yield limit.

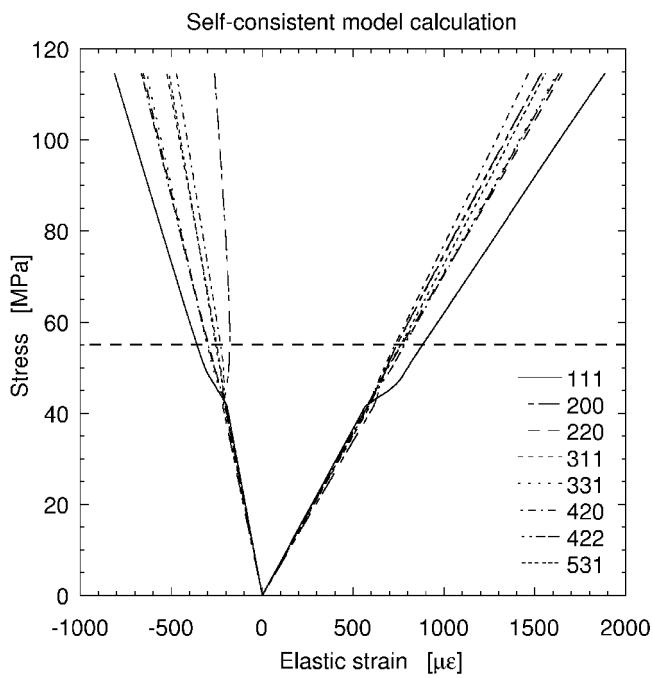

Fig. 4—Calculated elastic strains parallel and perpendicular to the tensile axis *vs* the applied stress. The horizontal dotted line shows the $\sigma_{0.2\ pct}$ yield limit.

the neutron measurements is based on the Hill–Hutchinson elastic-plastic self-consistent polycrystal deformation model.[11,12,13] In the model, the grains are regarded as ellipsoidal inclusions in a matrix with the integrated properties of the polycrystal. Plasticity is introduced as slip on the $\{111\}\langle 110\rangle$ slip systems in the fcc lattice. Using the initial critical resolved shear stress and hardening parameters, the model's macroscopic response is fitted to the measured macroscopic stress-strain curve obtained during the *in-situ* tensile test, as seen in Figure 2. Implementation of the modeling scheme and hardening law and general comparisons between the model and neutron diffraction measurements are described in Reference 14. In the model, a set of discrete grains, regarded as single crystals, is subjected to a far-field stress, and the resulting local stress and strain states for individual grains are iteratively determined. The calculations assumed a random texture, which is consistent with measurements on the sample. By extracting the elastic strains for grain sets that correspond to the reflections in the measurements, it is possible to compare the model predictions with the measured micromechanical response.

IV. RESULTS

The measured lattice strain evolution with applied load is shown in Figure 3. Data were recorded at ~20 MPa intervals, as illustrated for the 420 reflection parallel to the tensile axis. For clarity, the symbols are omitted for the other reflections and smooth line fits are displayed. The plot shows strains both parallel (positive) and perpendicular (negative) to the tensile axis. Parallel to the tensile axis, the spread in elastic strain is ~320 $\mu\varepsilon$ by the time the $\sigma_{0.2\ \mathrm{pct}}$ yield limit is reached. At or close to the $\sigma_{0.2\ \mathrm{pct}}$ yield limit, inflections for most of the reflections are apparent; however, the 111 reflection (shown in bold in Figure 3) crosses over the other reflections and exhibits an inflection at 80 MPa. The increase of the spread between the reflections is fairly uniform in the elastic and plastic regimes, and the reflections are fairly evenly distributed. Perpendicular to the tensile axis, the strain anisotropy of the reflections is less pronounced. Indeed, if the data for the 531 reflection are discounted (it was a weak peak with large errors), only the 200 reflection shows any appreciable deflection from the response of the other reflections.

Predicted elastic strains from the self-consistent model are shown in Figure 4. In contrast with the measurements, both parallel and perpendicular to the tensile axis, the elastic anisotropy below the $\sigma_{0.2\ \mathrm{pct}}$ yield limit is very small. Beyond the $\sigma_{0.2\ \mathrm{pct}}$ yield limit, the reflections parallel to the tensile axis exhibit a small strain anisotropy development, except for the 111 reflection, which shows a significant deviation. At the maximum load of 115 MPa, all but the 111 reflection are within a band of 190 $\mu\varepsilon$. Perpendicular to the tensile axis, the predicted strain anisotropy beyond the $\sigma_{0.2\ \mathrm{pct}}$ yield limit is notably larger than parallel to the tensile axis.

V. DISCUSSION AND CONCLUSIONS

The comparison between measured and predicted elastic strains shows that the model predictions agree relatively poorly with the measurements. Moreover, the measured anisotropy in the nominally elastic regime below the $\sigma_{0.2\ \mathrm{pct}}$ yield limit is surprisingly high. Pang *et al.*[5] found the elastic anisotropy of an Al7050 alloy to be much closer to the value expected. This indicates that the 2 pct magnesium in solution might have altered the elastic constants of the alloy compared to the pure aluminum. The calculated Young's modulus, assuming the single-crystal stiffnesses of pure aluminum, is 71 GPa, which is consistent with the literature values.[15] However, the measured macroscopic Young's modulus was 62 GPa, which is on the low side for aluminum alloys; this could, perhaps, indicate a disparity in the single-crystal elastic constants compared to those of pure aluminum used in the model. In the plastic regime, the development of the anisotropy is poorly predicted by the model. However, the shift for the 111 reflection from being the stiffest to being the softest parallel to the loading axis and *vice versa* perpendicular to the loading axis is seen in the model predictions, but not at the same load levels as in the measurements. Similar discrepancies above the $\sigma_{0.2\ \mathrm{pct}}$ yield limit were also observed in Reference 6 for commercially pure aluminum. However, for other fcc materials with higher elastic anisotropy, *e.g.*, austenitic stainless steel and copper, [7,16] comparisons between model and measurements showed much better agreement.

There are a number of possible explanations for the disparity between the model and measurements, as noted previously. The single-crystal elastic constants used in the model are for pure aluminum and the added 2 pct magnesium might have influenced their values. Prior plastic deformation of the material could have introduced residual stresses that can cause microyielding below the $\sigma_{0.2\ \mathrm{pct}}$ yield limit. However, the most obvious source of ambiguity is the evidence of DSA. None of the previous neutron diffraction studies on aluminum or aluminum alloys have reported evidence of DSA, and the results for Al7050 alloy[5] and commercially pure aluminum[6] show better agreement with model predictions. Plastic deformation during DSA can fall under two categories: temporal or spatial.[17] In the temporal regime (low plastic strains), the deformation is spatially homogeneous, but temporally heterogeneous, while in the spatial regime (high plastic strains), the deformation is both spatially and temporal heterogeneous. This was observed by McCormick[10] for strain-controlled tensile loading and Estrin *et al.*[17] for load-controlled tensile loading of a 6063 Al-Mg-Si alloy. Assuming similar conditions in our case would result in a spatial strain variation of about 0.1 pct within the neutron gage volume at 115 MPa.

In conclusion, the measurements on this system require further examination to address the implications of the DSA and to assess whether the single-crystal elastic constants used in the model are valid. Nevertheless, the results indicate that the self-consistent model (SCM) may have "problems" when the material has a low elastic anisotropy, *i.e.*, the anisotropic behavior is dominated by the plastic anisotropy alone. In the self-consistent model, the plastic deformation is modeled as multislip on the $\{111\}\langle 110\rangle$ slip systems. The effect of interaction between the slip systems during multislip in a polycrystal is not well documented, and in the present calculations, it is simplified by using an isotropic hardening matrix.[14]

ACKNOWLEDGMENTS

This work was supported, in part, under the auspices of the United States Department of Energy. The Manuel Lujan

Jr. Neutron Scattering Center is a national user facility funded by the United States Department of Energy, Office of Basic Energy Sciences—Materials Science, under Contract No. W-7405-ENG-36 with the University of California.

REFERENCES

1. D.J. Smith, R.H. Leggatt, G.A. Webster, H.J. MacGillivray, P.J. Webster, and G. Mills: *J. Strain Analysis*, 1988, vol. 23 (4), pp. 201-11.
2. G. Albertini, G. Bruno, B.D. Dunn, F. Fiori, W. Reimers, and J.S. Wright: *Mater. Sci. Eng.*, 1997, vol. A224, pp. 157-65.
3. R. Hermann: *Eng. Fract. Mech.*, 1994, vol. 48 (6), pp. 819-35.
4. M.J. Schmank and A.D. Krawitz: *Metall. Trans. A*, 1982, vol. 13A, pp. 1069-76.
5. J.W.L. Pang, T.M. Holden, and T.E. Mason: *Acta Mater.*, 1998, vol. 46 (5), pp. 1503-18.
6. B. Clausen and T. Lorentzen: *Metall. Mater. Trans. A*, 1997, vol. 28A, pp. 2537-41.
7. B. Clausen, T. Lorentzen, M.A.M. Bourke, and M.R. Daymond: *Mater. Sci. Eng. A*, 1998, vol. 259 (1), pp. 17-24.
8. M.A.M. Bourke, J.A. Goldstone, N. Shi, J.E. Allison, M.G. Stout, and A.C. Lawson: *Scripta Metall.*, 1993, vol. 29, pp. 771-76.
9. *Annual Book of ASTM Standards*, ASTM, Philadelphia, PA, 1998, vol. 01.05, p. 189.
10. P.G. McCormick: *Acta Metall. Mater.*, 1971, vol. 19 (5), pp. 463-71.
11. R.J. Hill: *Mech. Phys. Solids*, 1965, vol. 13, pp. 89-101.
12. R.J. Hill: *Mech. Phys. Solids*, 1965, vol. 13, pp. 213-22.
13. J.W. Hutchinson: *Proc. R. Soc. London A*, 1970, vol. 319, pp. 247-72.
14. B. Clausen, T. Lorentzen, and T. Leffers: *Acta Mater.*, 1998, vol. 46 (9), pp. 3087-98.
15. R.W. Hertzberg: *Deformation and Fracture Mechanics of Engineering Materials*, 4th ed., John Wiley & Sons, Inc., New York, NY, 1996, p. 7.
16. B. Clausen: Ph.D. Thesis, Risø National Laboratory, Roskilde, Denmark, 1997.
17. Y. Estrin, C.P. Ling, and P.G. McCormick: *Acta Metall. Mater.*, 1991, vol. 39 (11), pp. 2943-49.